コンクリート工学年次論文集, Vol.27, No.2, 2005

- Technical Paper -

A CODIFIED COMPARATIVE STUDY ON RC DEEP BEAMS BEHAVIOR WITH SMALL SHEAR SPAN TO DEPTH RATIO

Mohammad Reza SALAMY*1, Shigeki UNJOH*2 and Hiroshi KOBAYASHI*3

ABSTRACT

A comparative study on RC deep beams behavior is conducted in this paper by means of Japanese design codes (JSCE and JRA) prediction and finite element analysis and those results are evaluated by experimental observation. The beams have shear span to depth ratio between 0.5 and 1.5 and effective depth size from 400 mm to 1400 mm. Lateral reinforcement ratio varies by 0.0%, 0.4% and 0.8% in shear span. Estimated shear capacity by JSCE was around shear crack load while JRA code and Finite Element analysis have had closer results to experiment.

Keywords: RC deep beam, Shear failure, Shear span to depth ratio, Design code

1. INTRODUCTION

In order to investigate RC deep beams behavior and lateral reinforcement effects in improving shear behavior of those beams, a study is undergoing in Public Works Research Institute (PWRI) based on the experiments conducted during the year 2003 and 2004. Three sets of specimens comprise of nineteen RC beams including the experiments carried out on a joint research basis with Kyushu Institute of Technology (KIT) and Hanshin Expressway Public Corporation (HEPC) are investigated in this study. The beams have shear span to depth ratio between 0.5 and 1.5 and effective depth size from 400 mm to 1400 mm. The longitudinal tensile reinforcement ratio is kept almost constant in about 2% for all specimens while lateral reinforcement (stirrups) ratio varies by 0.0%, 0.4% and 0.8% in shear span. The results of experiment compared with Japanese design code such as Japan Road Association (JRA) [1,2] and Japan Society of Civil Engineers (JSCE) [3] as well as the finite element prediction. The results presented in this paper are part of a larger study on shear behavior of RC deep beams including size effect experimentally and numerically. It is found however that by increasing a/d in both design-codes, shear strength of the member will be decreased which agree well with experimental observation. On the other hand, JRA code yields better prediction in comparison with JSCE with an adequate safety margin. Furthermore, analytical investigation is adopted on JSCE proposed concrete constitutive model basis.

Table 1: Steel Properties of specimens

Beam	ρ_w %	ρ_{st} %	f_y MPa	Ast Asc	Stirrups
B-2	0.0	2.02	376	5D22 2D10	
B-3	0.4				D6@65
B-4	0.8				D10@75
B-6	0.0				
B-7	0.4				D6@65
B-8	0.8				D10@75
B-10-1	0.0				
B-10-2					
B-11	0.4				D6@65
B-12	0.8				D10@75
B-10.3-1	0.0	2.11	388	9D25 2D16	
B-10.3-2			371.7		
B-13-1	0.0	2.07	398	10D32 2D13	
B-13-2					
B-14	0.0	2.04	398	14D32 4D13	
B-17	0.4				D13@100
B-15	0.0	1.99	402	18D35 2D13	
B-16	0.0	2.05	394	18D41 2D13	
B-18	0.4		397.5		D16@120

*1 Dr. of Eng., Public Works Research Institute, Earthquake Engineering Team, JCI Member
*2 Dr. of Eng., Public Works Research Institute, Leader of Earthquake Eng. Team, JCI Member,
*3 Senior Research Engineer, Public Works Research Institute, Earthquake Eng. Team, JCI Member

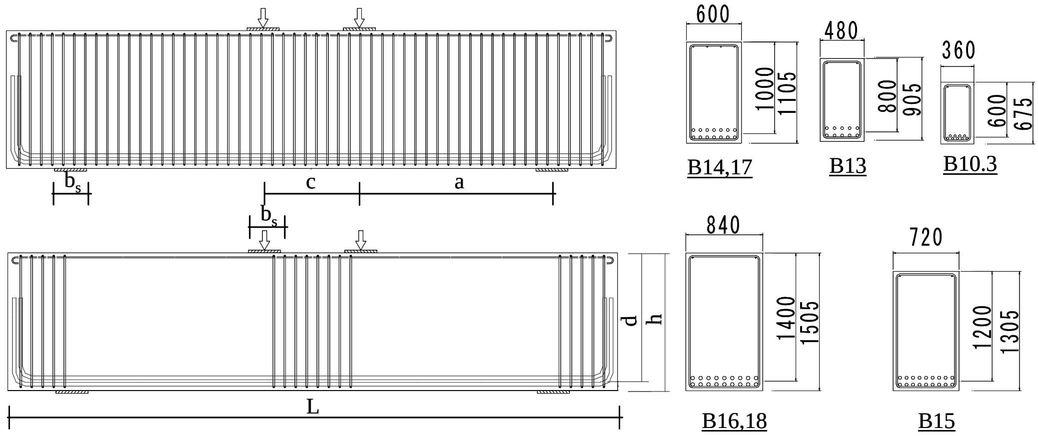

Fig.1. Detail of specimens with and without stirrups (unit: mm)

2. SPECIMENS GEOMETRIES AND MATERIALS PROPERTIES

To evaluate analytical results of FEM as well as code-based design, the following sets of experiments are carried out at PWRI and Kyushu Institute of Technology. However the complete analytical evaluation by FEM will be presented in some other publications and here only the results of design codes and a part of numerical calculation are evaluated by experimental evidences. Experiments consist of nineteen RC beams with geometric characteristic and material properties given in Fig.1, Table 1 and Table 2.

In Table 1, ρ_w, ρ_s, f_y, A_{st} and A_{sc} are shear span, stirrups ratio, longitudinal tensile reinforcement ratio and their yield stresses, cross section area of tensile and compressive reinforcement respectively. All specimens, with or without stirrups in shear span, have a minimum lateral reinforcement in mid-span and out of span. Despite absence of shear stress in this part, which at the first look implies un-necessities of shear reinforcement, they may delay or in some cases prevent the propagation of diagonal crack to the compression zone. It is believed even that reinforcements in mid-span sometimes are more efficient than those in shear span due to the reason stated above [4]. Further study is however necessary to confirm the effect of mid-span stirrups experimentally. In Table 2, b is specimen width, a/d and f_c' are shear span to depth ratio and

Table 2: Geometric and material Properties of specimens

Beam	a/d	Geometry size (mm)							f_c' MPa	P_u KN	P_{cr}^{sh} KN	δ_{peak} (mm)	Failure Mode
		L	c	a	d	h	b	b_s					
B-2	0.5	700	300	200	400	475	240	100	36.2	1550	525	3.16	All beams failed in shear (Mode II)
B-3										1536	625	4.78	
B-4									31.3	1951	700	1.85	
B-6	1.0	1100		400					31.3	1050	400	2.77	
B-7										1181	400	2.83	
B-8									37.8	1501	600	3.26	
B-10-1	1.5	1500		600					29.2	616	325	3.82	
B-10-2									23	703	278	5.28	
B-11									29.2	1025	350	15.96	
B-12									31.3	1161	300	7.05	
B-10.3-1		2250	450	900	600	675	360	150	37.8	1960	700	6.62	
B-10.3-2									31.15	1787	527	8.62	
B-13-1		3000	600	1200	800	905	480	200	31.63	2985	500	11.87	
B-13-2									24	2257	807	9.33	
B-14		3750	750	1500	1000	1105	600	250	31	3969	1100	9.27	
B-17									28.7	5214	1600	11.92	
B-15		4500	900	1800	1200	1305	720	300	27	5390	1500	11.91	
B-16		5250	1050	2100	1400	1505	840	350	27.3	5975	1900	10.57	
B-18									23.5	8396	2400	15.79	

concrete compressive strength. Maximum load capacity and related deflection as well as shear crack initiation load are denoted by $P_{\max}$, P_{cr}^{sh} and δ_{peak} respectively. Other geometrical parameters of Table 2 are schematically determined in Fig.1. All specimens are subjected to four points monotonic static load condition. Data acquisition of test is mainly focused on load- displacement relationship, mode of failure, crack patterns as well as steel and concrete strain in some designated locations to evaluate analytical results.

3. DESIGN CODES EQUATIONS FOR SHEAR STRENGTH OF RC MEMBERS

Design codes JSCE and JRA are employed here to predict tested beams load capacities and compare with experiment. Comparison is made by means of shear span to depth ratio as well as effective depth size effect. Since JRA code is not formulized like JSCE code and design values are presented in a tabular form, here only shear design procedure of JSCE is presented briefly.

JSCE code: Shear capacity of concrete in RC members V_{cd} (concrete contribution to shear capacity) is defined by the following equations. Parameters L and h are beam's span and height.

In case of $\frac{L}{h} \geq 2$ for simple beams:

$$V_{cd} = \frac{\beta_d \beta_p \beta_n \ f_{vcd} b_w d}{\gamma_b} \tag{1}$$

$$\beta_d = \sqrt[4]{\frac{1000}{d}} \leq 1.5 \tag{2}$$

$$\beta_p = \sqrt[3]{100\rho_s} \leq 1.5 \tag{3}$$

$$\rho_s = A_s / (b_w . d) \tag{4}$$

$$f_{vcd} = 0.2 \sqrt[3]{f'_{cd}} \leq 0.72 \quad (N/mm^2) \tag{5}$$

Parameters A_s , f'_{cd} , γ_b , b_w and d are longitudinal tensile reinforcements area, concrete ultimate compressive strength, material uncertainty parameter which in general case will be 1.3, member web width and effective depth in critical section respectively. Since the nominal shear strength is used for comparison with experiments, $\gamma_b = 1$ is supposed to set in all calculation. However the parameter for material uncertainty is not explicitly stated in JRA code therefore to have a meaningful comparison between two codes $\gamma_b = 1.3$ is conducted. On the other hand experimental results are also calibrated by the same reduction factor equal to 1.3. The value $\beta_n = 1$ is also adopted due to the code definition for simply supported beams.

In case of $\frac{L}{h} < 2$ for simple deep beams:

$$V_{cd} = \frac{\beta_d \beta_p \beta_a \ f_{dd} b_w d}{\gamma_b} \tag{6}$$

$$f_{dd} = 0.19 \sqrt{f'_{cd}} \quad (N/mm^2) \tag{7}$$

$$\beta_a = \frac{5}{1+(a_v/d)^2}, \quad a_v = a - b_s / 2 \tag{8}$$

$$\phi = -0.17 + 0.3(a_v / d) + 0.33 / \rho_{wb} \leq 1.0 \tag{9}$$

$$V_{sdd} = \phi . V_{sd} \tag{10}$$

$$V_{sd} = \frac{A_w f_{wyd} (\sin\alpha_s + \cos\alpha_s) / s_s}{\gamma_b} . z \tag{11}$$

where b_s is support length (Fig.1), the internal lever arm $z \approx d / 1.15$ and design yield strength of shear reinforcements $f_{wyd} \leq 400 MPa$ for normal strength concrete. Parameters β_a and ρ_{wb} are shear span ratio's effect and shear reinforcement ratio respectively. Lateral reinforcement contribution to shear capacity is denoted by V_{sd} and is calculated by Eq.11 for any values of $\frac{a}{d}$ ratio. Finally the shear capacity of entire section V_{yd} is calculated through Eq.12 as below.

$$V_{yd} = V_{cd} + V_{sdd} \tag{12}$$

4. COMPARISON OF THE RESULTS

Both codes are applied for shear load capacity calculation. The results of codified calculation and experiment are shown in figures of this section.

4.1 Load capacity

As mentioned in section 4, only beams with L/h<2 are considered as deep beam by JSCE design code. In other words despite most other design codes including JRA which recognize beams with a/d<2.5 as deep beam, only the specimens tested in this study with a/d=0.5 are recognized by JSCE code as deep beam. Nevertheless in this study, beams are designed in both cases of only following JSCE regulation as well as considering all specimens as deep beams and applying JSCE deep beam criterions. Figures 2 and 3 show ultimate loads of specimens along with those obtained by the aforementioned design codes. Dotted lines in figures illustrate reduced specimens ultimate loads by means of JSCE reduction factor $\gamma_b = 1.3$ to calibrate test results for the sake of comparison with reduced design codes predictions.

As can be seen in both figures, JRA code gives much better agreement to the experiment than JSCE code with an acceptable safety margin. JSCE code however seems not so consistent in terms of deep beam definition and the results show a kind of scatter distribution around both solid and dotted lines. It is also observed that no data points fall significantly below either line for any of the codes. Experiment showed that shear crack initiated at about 40% of the ultimate load. This crack will be extended to entire shear span (full shear crack) at about $0.5P_u$. Consequent to load increase, arch action will maintain load capacity of the beam up to about 80-90% of the ultimate load. Afterward shear cracks are severely widened and extended to compressive zone where shear sliding of concrete pieces around shear crack could be clearly observed with even bare eyes. This point is practically considered the ultimate capacity of beam in shear by a number of design codes, which the beam is in serious irreversible circumstances. Aggregate interlock is almost exhausted in this stage and beam enters to its failure process. Figure 3 shows data points obtained from code prediction and test results.

The figure shows that JSCE code have usually estimated the load capacity of members around shear crack initiation load while JRA code yields the results near practical ultimate capacity of beams (about 0.8Pu). In other words, JRA allows shear crack occur and extend but JSCE allows only shear crack form but not extend. It is acceptable in essence if the philosophy of JSCE code like some other design codes is to ensure the safety of structures before initiation of shear cracks not to reach to the ultimate load. Nevertheless the discrepancy in the results is for beams with a/d<1.0 which gave rise to a jump in predicted shear capacity of the member by JSCE and despite a big safety margin for specimens with larger a/d ratio, these beams seem to be overestimated. For a/d=0.5, JSCE and JRA yield almost same prediction but the more a/d increases the more codes predictions differ.

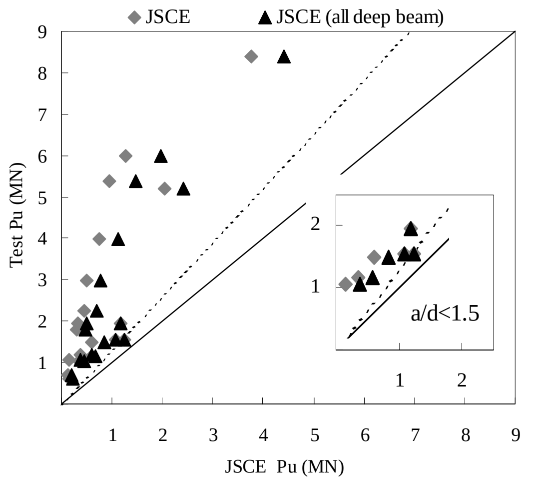

Fig.2. JSCE code P_{max} versus test result

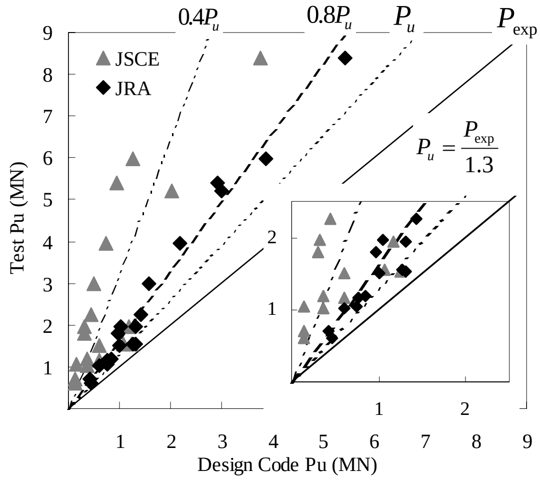

Fig.3. Codes ultimate load versus test

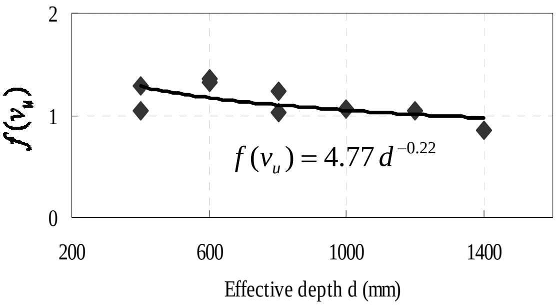

Fig.4. Effective depth versus shear function $f(v_u) = V_u / bd\sqrt[3]{f'_c}$ for Av=0 and a/d=1.5

4.2 Size effect

In order to study size effect in shear capacity of beams with low a/d ratio, both code examined and verified with experimental results. Test specimens cover a wide range of effective depth from 400mm to 1400mm. Accordingly variation of average shear stress taking into account concrete compressive strength ($V_u / b.d.\sqrt[3]{f'_c}$) in terms of effective depth is shown in figure 4. To eliminate a/d effect on ultimate shear stress of the beams, only a/d=1.5 is considered here. It is clearly seen that as long as the effective depth increases, the shear strength of the section decreases. The regression curve is assumed to be a power function of effective depth d in order to adjust to the size effect function proposed by JSCE and JRA. The equation is round off and rewritten as:

$$f(v_u) = \lambda (d^{-0.22}) \qquad (13)$$

where coefficient λ is a function of a/d ratio,

reinforcement ratio and member's boundary condition. Since the three aforementioned parameters are constant for the beams used for producing figure 4 consequently $\lambda = 4.77$ is determined to fit the best to experiment data points. According to JSCE, shear strength varies in a form given by Eq.2 in terms of $d^{-\frac{1}{4}}$. On the other hand JRA proposed procedure can be estimated by a function of $d^{-\frac{1}{3}}$ to take into account size of specimen. Although the foregoing expression of figure 4 is a crude approximation, the form of Eq.13 agrees well with that of Eq.12 of JSCE code. It is however not a significant differences between JSCE and JRA size effect expression as can be seen in Fig.5 and both expressions are attributed to a reasonable estimation of member depth effect.
The maximum values for this coefficient set to 1.0 and 1.5 by JRA and JSCE respectively. In essence JSCE attributes 50% increase in shear strength to size effect while JRA does not allow any increase in shear strength. This is rational due to the fact that JRA is usually dealing with structures with large components most of them larger than one-meter depth but JSCE is likely considered as a general design code for wider range of structures.

5. FINITE ELEMENT SIMULATION

In order to evaluate JSCE proposed constitutive model in FEM application and also to conduct parametric study on a larger number of specimens for future works, specimens B2, B6, B10-1, B10.3-1, B11, B14, B15, B16 and B18 are selected as representative specimens for analysis. They cover all a/d ratios adopted in the experiment. The constitutive behavior of concrete is represented by a rotating smeared crack model. Elastic-perfect plastic model is assumed for all reinforcing bars with zero shear strength.

Concrete constitutive models are assumed in a fracture type material basis with a characteristic length parameter. This assumption accomplishes a mesh objective analysis particularly by taking into account energy released in fracture process irrelevant to the mesh discretization. Material models suggested by JCSE are employed here for numerical modeling and shown in Figs. 6 and 7. In compression model, $k_1 = 1$ is adopted for all analyses and fracture energy in tension is based on JSCE definition represented in Eq.14.

$$G_F = 10\,(d_{\max})^{1/3}\, f_c'^{\,1/3} \qquad (14)$$

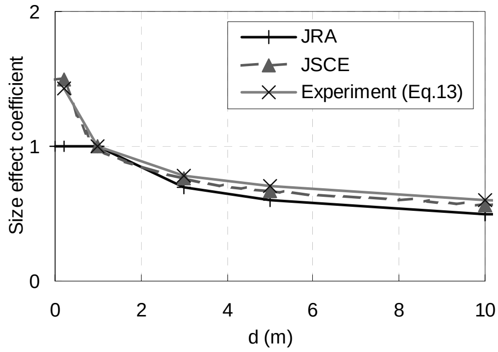

Fig.5. Effective depth versus size effect coefficient

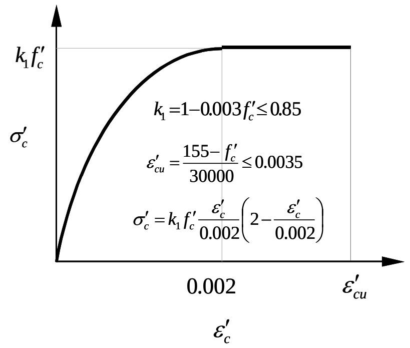

Fig.6. Concrete Compressive model

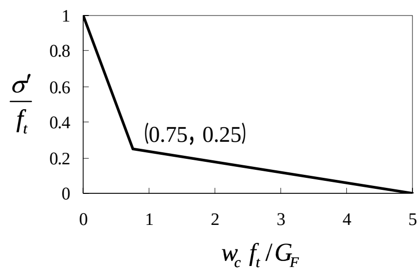

Fig.7. Concrete Tension model

where d_{max} is maximum aggregate size in mm and G_F is fracture energy in N/m. Figure 8 shows analytically obtained peak load versus experiment. Predicted peak loads are in average about 70% of test load capacity which is much clearly depicted in Fig.9. This figure gives better estimation of analyses precision particularly for the specimens with lower load capacity. It is noteworthy to mention that the lesser a/d ratio the higher possibility of compressive stress reaches to concrete compressive strength. Looking at one of the load-deflection results (Fig.10), it implies that if concrete compressive stress could be maintained by for instance means of smooth softening path, sudden drops of load could be avoided and the results would be much closer to experiments. In this regard some modification in compressive constitutive model such as linear stress softening ought to be necessary. All beams of this study however are analyzed with different material models and will be appeared in further publication[5]. Better agreement with experiment has been obtained in the latter case due to more rational concrete post peak compressive model.

6. CONCLUSION

A comparative study between experiment, JSCE and JRA design codes as well as FE analysis in terms of ultimate loads, shear crack loads as well as size effect issues is carried out and following conclusions are drawn.

1. It is found that JRA code has a consistence design procedure for RC beams with low shear span to depth ratio. Due to deep beam assignment by either codes, JRA assigns all beams as deep beam while only beams with a/d=0.5 of this study fit to deep beam criterion of JSCE. On the other hand since deep beams usually have higher shear strength due to the resisting mechanism and in fact all beams of this investigation are following such resisting mechanism (arch action), there will be a clear discrepancy between test results and predicted strength by JSCE code. Estimated shear load capacity by JSCE is around test shear crack load while JRA code allows shear cracks form and extend to a certain level (about $0.8P_u$). In this sense it can be concluded that JSCE yields much conservative results than that of JRA except for very small a/d ratio say 0.5 where JSCE amplifies the predicted shear strength by means of a function of a/d ratio.

2. Size effect on shear strength of RC beams with low a/d ratio is adequately included in either code. The main difference between the codes lies on the beams with depth smaller than 1000mm which JRA limits the coefficient to one but JSCE goes as far as 1.5 and attributes shear strength to the size effect up to 50% higher at the most.

3. Finite element analyses of selected beams have been in average about 70% of specimens load capacity due to the several sudden drops in load-deflection response. One reason out of others might be relevant to sudden stress drop after maximum compressive stress in the proposed constitutive model by JSCE. Further concern seems to be necessary to modify stress-strain model after peak compressive stress.

ACKNOWLEDGEMENT

A part of experimental data used in this study was provided by Prof. Kenji Kosa from Kyushu Institute of Technology and Dr. Tsutomu Nishioka from Hanshin Expressway Public Corporation respectively. Their kind help is gratefully acknowledged.

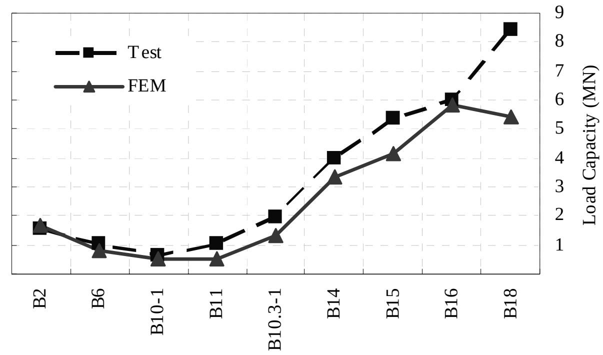

Fig.8. Test and FEM Ultimate Load (MN)

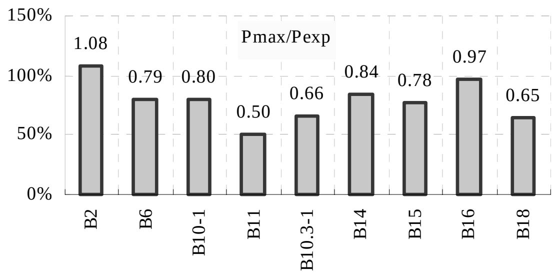

Fig.9. FEM predicted P_{max} to test P_{exp} ratio

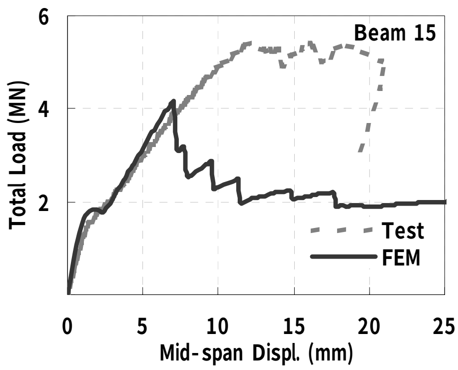

Fig.10. Beam 15 test and FEM prediction

REFERENCES

[1] Japan Road Association. Design Specifications of highway bridges. Part IV; 2002.

[2] Japan Road Association. Design specifications of highway bridges. Part V; 2002.

[3] Japan Society of Civil Engineers. Standard specifications for concrete structures, Structural performance verification. 2002.

[4] Behavior of Reinforced Concrete Beams with a Shear Span to Depth Ratio Between 1.0 and 2.5, M. D. Kotsovos, ACI, May-June 1984.

[5] Experimental and Analytical Study on RC Deep Beams Behavior, M. R. Salamy *et al.*, Concrete and Development Conference, Iran, April 30-May 2, 2005 (to be appeared).